Development of a Fracture Mechanics Methodology to Assess the Competing Mechanisms of Beneficial Residual Stress and Detrimental Plastic Strain Due to Shot Peening

Marsha K. Tufft
General Electric Aircraft Engines
Cincinnati, Ohio, U.S.A.

ABSTRACT

The results from a shot peen Design of Experiment (DoE) conducted a few years earlier suggest that competing mechanisms of beneficial residual stress and detrimental plastic strain and surface roughness may control the low cycle fatigue behavior of shot peened specimens. In order to better understand the mechanisms at work, several coupons were shot peened to a subset of the conditions studied in the DoE. Residual stress and plastic strain distributions were obtained using X-ray diffraction techniques. Microstructural evaluation of the specimens included: microstructures etched to reveal slip character as a function of depth below the peened surface, energy dispersive spectroscopy (EDS) to reveal surface chemistry, Auger spectroscopy on selected coupons to determine surface chemistry with depth profile, surface roughness and hardness measurements, determination of weight loss due to shot peening (erosion), and high resolution SEM observation on one electropolished specimen to look for the presence of microcracks. As a result of this effort and a related investigation studying the single particle impact of production shot [1], a fracture mechanics method was developed to provide an estimate of the lower bound life capability of shot peened material. Although a limited number of test conditions have been evaluated to date, the results are encouraging and merit further investigation.

Key Words: Peening, Shot Peening, Fracture Mechanics, Residual Stress, Plastic Strain

I. Introduction

The beneficial effects of shot peening have long been recognized. One of the major reasons for shot peening has been to induce a beneficial compressive stress layer that acts to retard the propagation of cracks from surface features. If crack initiation and propagation from surface features can be suppressed, longer component operating lives can often be attained. Although Luetjering, Wagner [2], and others have long recognized that shot peening can also cause the equivalent of fatigue damage, this effect has received considerably less attention.

A major goal of the current effort is the development of a method to quantify the effects of these competing mechanisms. The fracture mechanics method developed appears to provide a reasonable lower-bound prediction of life capability due to shot peening for the powder-metal Nickel-base alloy, René 88DT, which was used in the investigation. Additional work is needed to validate the method. This paper describes the effort to date, and some of the data supporting the application of a fracture mechanics approach.

Figure 1 – Shot Peen Design of Experiment (DOE) Summary

Average life values given in standard deviations from average LCF life (calculated on log scale).

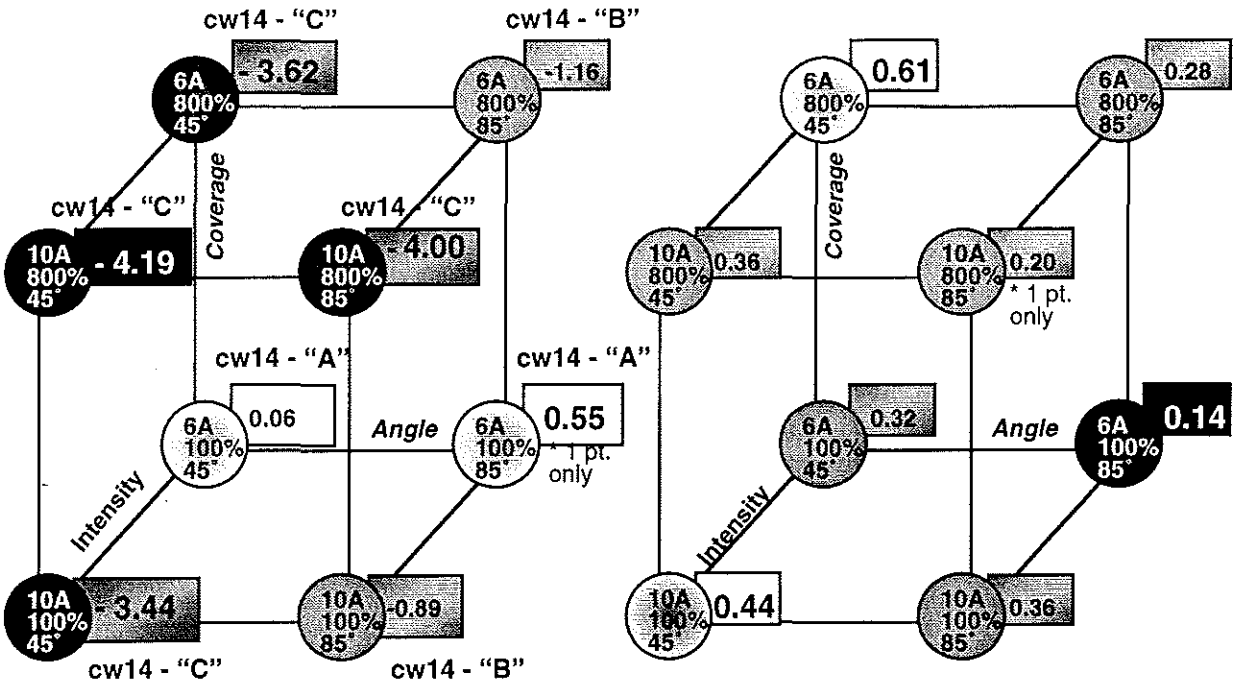

a) CCW14 SHOT PEEN DOE

b) CCW31 SHOT PEEN DOE

Best condition: **low** intensity, **low** coverage, **high** angle.
Lowest life condition: **high** intensity, **high** coverage, **low** angle.
Statistically significant differences. Groupings "A", "B", "C" shown are those used in Weibull analysis (Figure 2).

Robust process. **NO STATISTICALLY SIGNIFICANT differences between effects.** All ccw31 data were analyzed as one population for Weibull analysis (Figure 2).

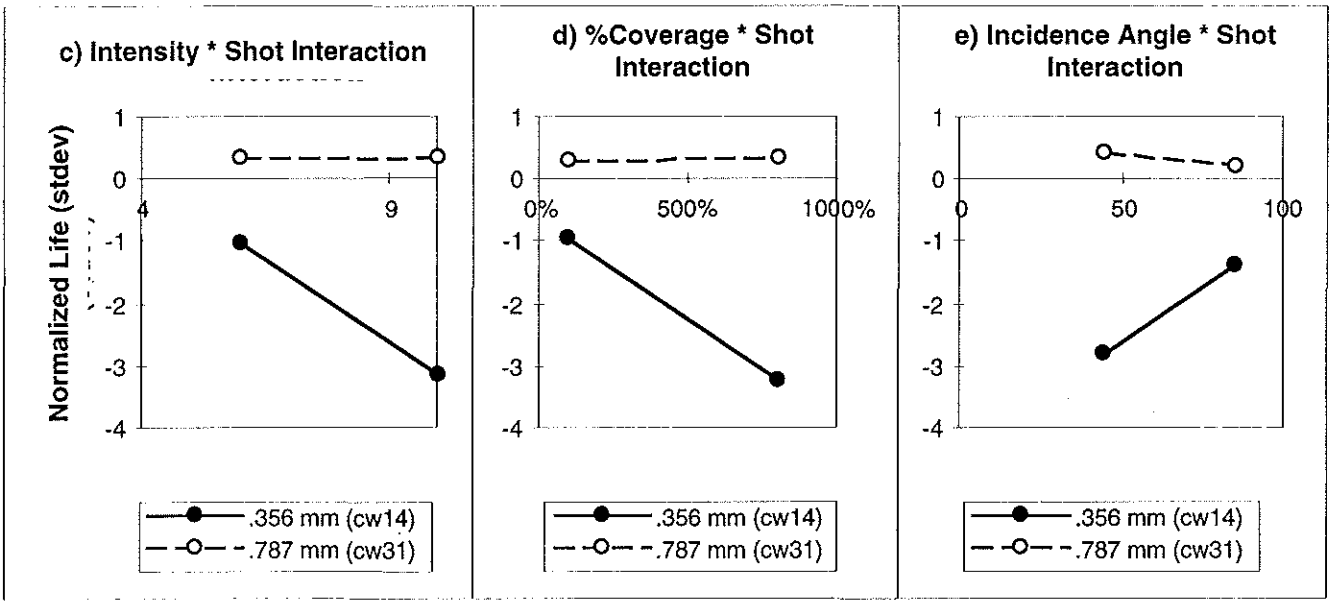

Main effects & interactions which are significant at the 95% confidence level: 1) shot (Pr>F=.0001), 2) shot*coverage (Pr>F=.0003), 3) coverage (Pr>F=.0005), 4) shot*intensity (Pr>F=.0015), 5) intensity (Pr>F=.0018), 6) shot*incidence angle (Pr>F=.0038), 7) incidence angle (Pr>F=.0161), 8) shot*coverage*intensity*angle (Pr>F=.0446), 9) coverage*intensity*angle (Pr>F=.0498). Normalized lives with arcsine trasnsformation used for analysis. Lives quoted above represent represent the number of standard deviations of LCF life from average, for the stress and temperature conditions of the test.

II. Results of the Shot Peen Design of Experiment (DoE)

Several years ago, a shot peen DoE was conducted by Bailey[3] to evaluate the effect of shot peening on low cycle fatigue (LCF) life. A total of four factors were evaluated at two levels each as shown in Table 1, for a total of 16 different peening conditions. Each condition was replicated twice, for a total of 32 tests. Standard smooth round bar specimens, 0.4" in diameter were used. The tests were run at 1000°F, at a stress level chosen to yield an average life of 100,000 cycles for low-stress ground specimens.

Table 1: Summary of Factors Evaluated by Shot Peen Design of Experiment

	Factor	Low Level	High Level
1	Shot	CCW14 (.014" dia)	CCW31 (.031" dia)
2	Intensity	6A	10A
3	Incidence Angle	45°	85°
4	% Coverage	100%	800%

Notation: Intensities of 6A and 10A refer to the arc height deflection of an Almen "A" strip in thousandths of inch, i.e. .006" and .010" deflection. Coverage is determined by a visual inspection. "100%" coverage represents approximately complete coverage of the Almen strip by peening dimples. "800%" coverage is achieved by peening each specimen 8 times longer than that necessary for 100% coverage. Four point saturation curves are run to verify that the selected "100%" coverage point meets the criteria of the intensity measurement definition (increasing the exposure time by 2X results in less than a 10% increase in arc height deflection). Incidence angles represent the angle between the target surface and direction of incoming shot. Thus 90° represents a normal impact (perpendicular to the surface) and 45° represents an oblique impact. The shot used are CCW14 and CCW31, conditioned cut-wire shot of approximately .014" and .031" diameter respectively.

Results. Some of the key results are presented in Figure 1. Life results are represented in normalized form as the number of standard deviations from the average life of a low stress ground bar, calculated on a log scale. Figure 1 shows the test results and some of the key interactions. Figures 1a and 1b are cube plots, which show the average lives for each condition plotted on axes of angle, coverage and intensity. Figures 1c, 1d, and 1e show the significant two-factor interactions. As can be seen from these results, the larger ccw31 shot produced "good" lives (greater than or equal to the average life of low-stress-ground specimens at the same test conditions) over the entire range of conditions evaluated, while the smaller ccw14 shot produced good lives at low intensity / low coverage conditions. The smaller ccw14 shot produced "low" lives (lives which are significantly lower than average lives obtained for low-stress-ground specimens) at high intensity / high coverage conditions. Oblique incidence angles of 45° were more detrimental to life than nearly normal 85° incidence angles, as the 6A/45°/800% condition had consistently low lives, whereas the 6A/85°/800% results were mixed. This was also evident with the 10A/45°/100% condition (low lives) when compared with the 10A/85°/100% condition (mixed results). Use of an arcsine transformation further improved the resolution of the analysis.

Figure 2: Weibull Analysis Results

(1000˚F, stress level chosen to give 100,000 cycle nominal life)

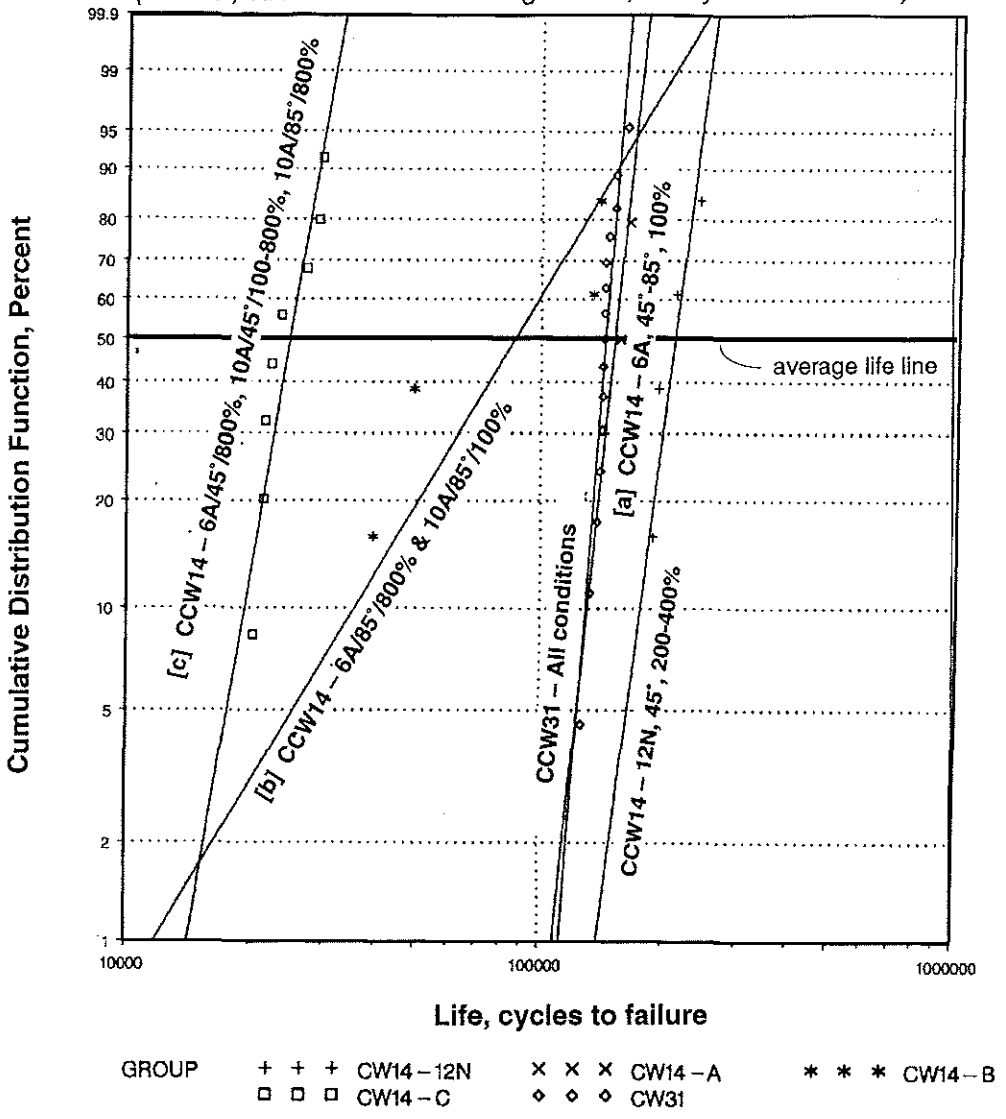

2 Parameter Weibull Analysis Results of Shot Peen DOE data (SAS software, maximum likelihood)

symbol	SHOT	GROUP	(average life) **SCALE**	(failure mode) **SHAPE**	Interpretation of SHAPE factor	**std. error** SHAPE	SCALE
+	CW14	12N45	220,353	10.01	rapid wear out	11,696	3.79
×	CW14	A	155,845	12.80	rapid wear out	7,352	6.51
*	CW14	B	102,808	2.13	LCF (mixed-modes)	25,489	0.89
□	CW14	C	25,891	7.71	rapid wear out	1,259	2.12
◇	**CW31**	ALL	146,672	17.48	rapid wear out	2,302	3.15

3 Parameter Weibull Analysis Results of CCW31 data (Weibull-Smith software, rank regression)

symbol	SHOT	**Threshold**	**SCALE**	**SHAPE**	Interpretation	R^2
◇	**CW31**	-333,308	479,694	71.45	Significant damage accumulated (due to shot peening) prior to test.	1.0

II. Weibull Analysis of Shot Peen DoE Results.

A Weibull analysis was also conducted, as illustrated in Figure 2. For this analysis, all the ccw31 data points were analyzed together as one group. The ccw14 data points were grouped into three groups, as characterized by their life behavior and identified in Figure 1. In addition, the results from four ccw14/12N/45° tests at 200-400% coverage were included as a separate population. 12N, light peening, is the approximate equivalent of 4A intensity.

The cumulative distribution function for the Weibull distribution [4] is given as:

$$F(t) = 1 - e^{-((t-t_0)/\eta)^{\beta}} \qquad (1)$$

where t is the life, t_0 is a threshold parameter which applies only to a three-parameter Weibull, β is the shape parameter and η is the scale parameter.

The slope factor from the Weibull analysis can be used to indicate the type of failure mode (slope <1 = infant mortality, slope=1 => random, slope=2-3=>LCF, slope>5=>rapid wear out). The 50% line gives the average life (also the scale factor). The average lives for the peened ccw31 specimens are not significantly different than for low stress ground specimens, but the slopes are much steeper (indicating rapid wear out mode), thereby resulting in lower variation (and higher -3σ lives). This suggests that shot peening reduces the crack initiation time (by accumulating plastic strain, which is equivalent to fatigue damage); however it also increases the crack propagation life due to the beneficial residual stress layer imparted. This is another way of describing the effects of competing mechanisms of beneficial residual stresses vs. detrimental plastic strain. The ccw14 population "C" - "low" lives - show a similarly steep slope, but the curve is shifted to the left by nearly one order of magnitude. Thus, more damage is accumulated leaving less crack propagation life remaining. The ccw14 population "A" - good lives - is virtually indistinguishable from the ccw31 curve. The ccw14 - 12N light peened curve is further to the right, suggesting that light peening does even less "detrimental plastic strain damage" resulting in higher average lives in the absence of any surface inclusions. There is other data which suggests that "light peening" does not provide the same level of protection when a surface defect is present. More work is needed to understand the limits of light peening in the presence of defects. The fit obtained for the population "B" - the transition in mechanisms - is relatively poor and reflects the high amount of variability in lives for these specimens.

The results of a 3 parameter Weibull analysis on the ccw31 data show a negative t0 (threshold) value. If this analysis is valid, it indicates that a significant amount of the total life capability (about 70%) is consumed by peening; however because of the beneficial effects of the residual stresses, the total life capability is increased by ~480% over low stress ground (LSG) specimens. The net effect is an average life which is slightly higher than that of average LSG specimens (146,000 vs. 100,000). The 3 parameter Weibull analysis is a non-linear analysis and requires a minimum of about 14 data points to yield significant results. It appears to be sensitive to initial values used to start the parameter estimates, so it is possible to find either positive or negative solutions with varying goodness-of-fit characteristics. The analysis conducted resulted in a perfect R^2 regression correlation coefficient of 1.

Figure 3: Sample Residual Stress Profiles and Corresponding Curve Fits

Measured intensity & curve fit intensity given in parentheses: [measured, curve fit]

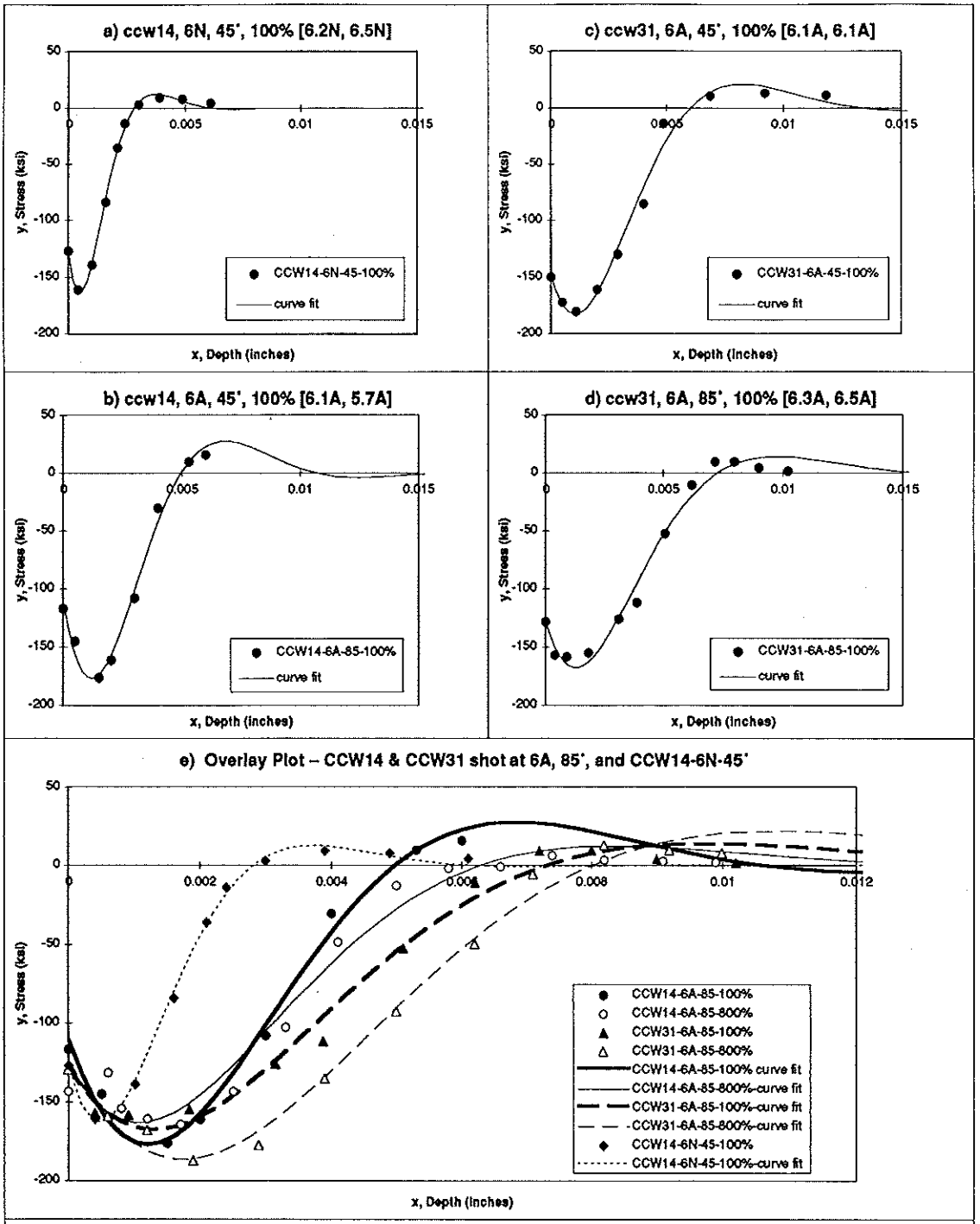

Comparison of residual stress profiles obtained by x-ray diffraction. Eight point saturation curves were obtained for these conditions, and a regression analysis performed to fit a curve of the form: intensity=A*exp(-B/T) where T is exposure time , A and B are regression constants. This equation was then solved to determine the intensity which satisfies the requirement that doubling the exposure time yields a 10% increase in intensity. An alternate form, intensity=A*exp(-B/T)+CT^2, is used when 4T and 8T points show continued rise in intensity with increasing time. The regressed intensities will be given below for comparison purposes vs. standard definition of intensity.

a) ccw14, 6N(2A), 45°, 100% - curve fit intensity=6.5N. b) ccw14, 6A, 45°, 100% - curve fit intensity=5.7A. c) ccw31, 6A, 45°, 100% - curve fit intensity=6.1A. d) ccw31, 6A, 85°,100% - curve fit intensity=6.5A. e) overlay plot shows that ccw31 curves do show slightly deeper residual stress profiles consistent with the curve fit intensity of 6.5A versus 5.7A for ccw14 shot. Using the existing definition of intensity, these curves were identified as having intensities of 6.3A (ccw31) vs. 6.2A (ccw14).

III. Material Changes induced by Shot Peening

Some of the effects of shot peening, as reported in the literature [5, 6], include:

- Beneficial compressive residual stresses at the surface
- Balancing tensile residual stresses subsurface and shear lag
- Work hardening of the surface layers (increase of plastic strain)
- Erosion
- Massive phase transformations
- Increased surface roughness
- Decreased ductility
- "Cleaning" of the surface layer (removal of oxide films, etc.)
- Adiabatic heating due to impact
- Material transfer (embedding of glass shot fragments, transfer of iron)
- Deformation - warping or bending - of thin sections

To quantify these effects, the following microstructural/metallurgical evaluations were conducted:

- X-ray diffraction to determine residual stresses and plastic strain profiles
- Optical and SEM microstructures of peened specimens
- High resolution SEM observation of one specimen, to look for microcracks
- Surface roughness measurements using WYKO laser interferometry profiler
- Surface hardness measurements
- Energy dispersive spectroscopy (EDS) surface chemistry analysis
- Auger spectroscopy analysis of surface
- Measurement of specimen weight loss due to peening (to quantify erosion effects)

Compressive Residual Stresses. Figure 3 shows a sample of the compressive residual stress profiles, and the accompanying curve fit used to provide input for the fracture mechanics analysis. For the 6A intensity conditions shown, use of ccw31 shot results in slightly deeper residual stress profiles. However at other intensities, the profiles are more closely bunched. Linear regression analysis of a large number of x-ray diffraction profiles indicates that the depth of the compressive stress layer is very nearly a linear function of intensity alone. However, the definition of intensity per MIL-S-13165C [7] does not provide a unique, unambiguous definition to differentiate between peening conditions. Thus, some of the variability observed in life data and in residual stress profiles may be due to variations between the interpretation and determination of intensity.

Based on prior work by VanStone [8], experience shows that good curve fits to residual stress profiles can be obtained by using an exponential*sine function of the form:

$$\sigma = A \cdot e^{-x/\lambda} \cdot \sin(B \cdot x + C) \qquad (2)$$

This is a simpler form of the equation for stress as a function of depth for Rayleigh waves. The Rayleigh wave is a surface wave, and is the primary stress wave form active in erosion by small particles as noted by Hutchings [9], Henning and Mewes[10]. The presence of Rayleigh waves was also noted in the single particle impact experiments conducted in conjunction with this effort. Although Rayleigh waves are known as elastic surface waves, there is no reason why a plastic Rayleigh wave could not also exist, similar to longitudinal

Figure 4: Comparison of Sample Plastic Strain Profiles

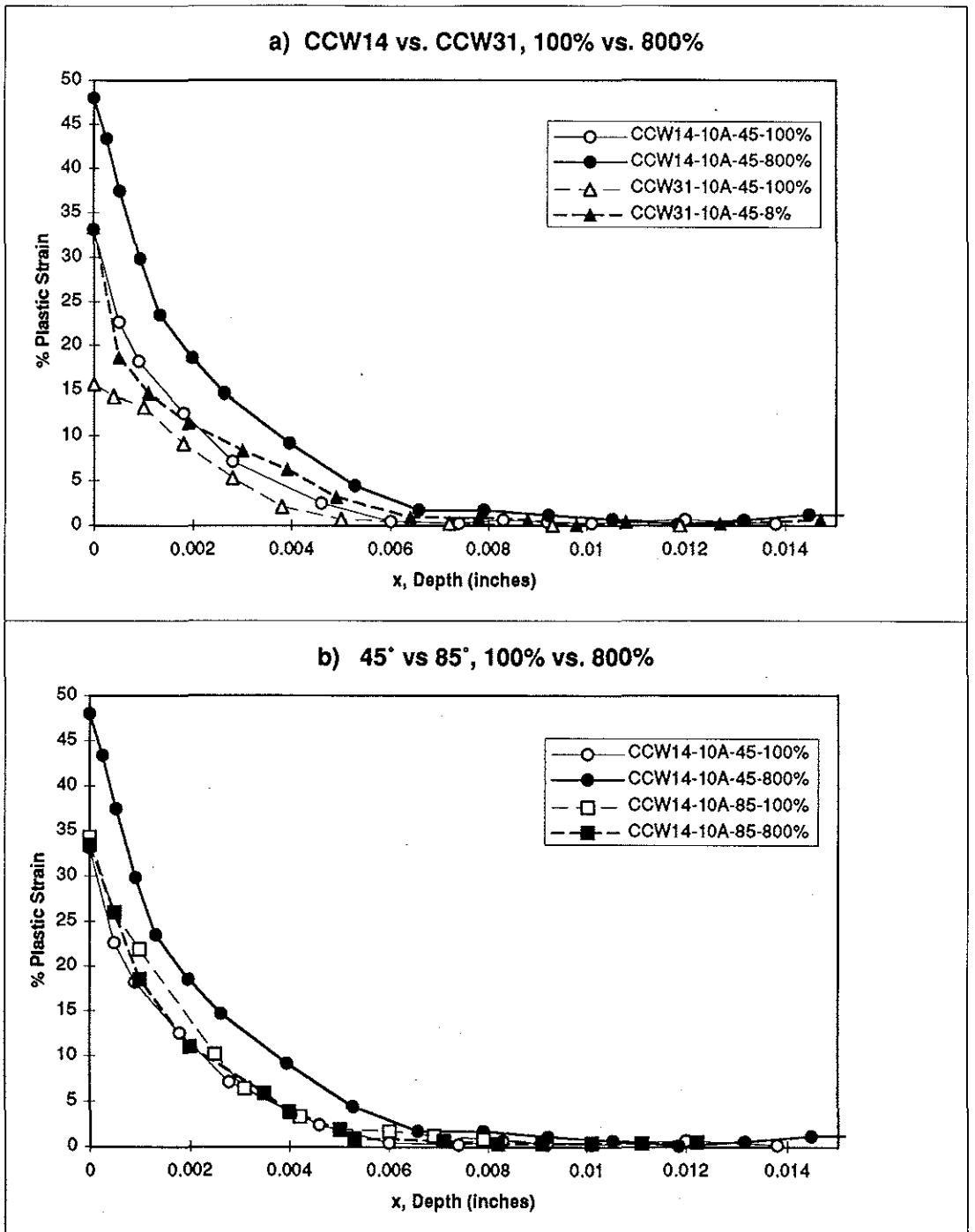

a) plastic strain distributions for ccw14 vs ccw31 shot at 10A/45°/100% & 800% coverage. Note that the ccw31/100% profile is significantly lower than the others, while the ccw14/800% is the deepest. The ccw14/10A/100% and ccw31/10A/800% profiles are similar. For a given intensity, small shot will induce greater plastic strains than larger shot.
b) plastic strain distributions for 45° vs 85° for ccw14/10A/100% & 800%. At 85°, plastic strain did not increase substantially between 100% and 800% coverage. At 45°, amount of plastic strain does increase substantially between 100% and 800%. Curve fit intensities: ccw14/10A/45° - 9.5A; ccw14/10A/85° - 9.0A; ccw31/10A/45° - 9.6A.

and shear waves which can have elastic precursors followed by a plastic wave. A key characteristic of the Rayleigh wave is that it decays exponentially with depth, describing the residual stress profile very well. It would also explain the shape and formation of the lip around a dimple that occurs at high strain rates. Thus, it is possible that a physical mechanism, the Rayleigh wave, is involved in the development of the residual stress profiles.

Plastic Strain Profiles. Figure 4 shows a comparison of plastic strain profiles: 4a compares the effects of smaller ccw14 shot versus ccw31 shot at 10A/45°/800%; 4b compares the effects of 45° versus 85° incidence angle at ccw14/10A conditions. The magnitude of the peak plastic strain value is significantly higher (order of 2X) for the small shot compared with the larger ccw31 shot. For a given intensity, the 45° incidence angle results in significantly greater plastic strain magnitude and depth at the 800% coverage condition.

Erosion. To determine if erosion is a significant factor in life behavior, residual stress coupons (nominal dimensions 3" x .75" x .25" thick) were weighed before and after peening. Significant erosion is observed for the most damaging life conditions. Erosion (mass loss) is greatest for the 45° incidence angle / 800% coverage condition. This is consistent with erosion behavior of ductile metals, for which the greatest erosion occurs at low incidence angles, the least at normal (85°-90°) incidence angles [11]. Whether the amount of erosion is a causative factor or correlating factor is unclear. It seems more likely that presence of significant erosion is characteristic of extreme plastic strain accumulation damage. Erosion is not just cutting and ploughing of metal by contact, it is also spalling of metal due to fatigue by repeated impacts.

Surface Roughness. Surface roughness measurements were taken with a WYKO laser interferometry profiler, which also produced surface statistics necessary for calculating a surface roughness Kt. Surface roughness increases with 1) higher intensity 2) decreasing incidence angles, 3) decreasing shot size. It decreases with increasing % coverage.

Adiabatic Heating. Transmission Electron Microscopy (TEM) analysis of two peened specimens revealed evidence of recrystallization at the surface [12]. This effect was also noted and reported by Renzhi [13]. Recrystallization would require significantly high transient temperatures due to impact. As part of the single particle impact experiments conducted in conjunction with this effort, high temperatures were successfully measured for a few tests. Temperatures were on the order of 350°C, and lasted 20-300 μs. This was an extremely difficult experiment due to the small sensor array area and the difficulty in aiming shot precisely enough to land on the area being sensed. The conditions successfully measured did not represent the high strain rate conditions attained by the small ccw14 shot at 10A intensity. Nor could it account for the possibility of "shocking-up" effects, or the interaction between multiple impacts. But it did confirm the generation of significant heat at impact, suggesting that localized recrystallization (depth of .0002") could be induced by the impact event due to frictional heating. This suggests that less heating would occur for normal impacts than for oblique impacts.

Material Transfer. Energy dispersive spectroscopy (EDS) and Auger spectroscopy was performed on selected residual stress coupons. This analysis confirmed the presence of iron only on specimens corresponding to the low life results. Since presence of erosion was

confirmed, it is likely that material is being eroded and/or spalled from both target and shot. At high strain rates, adiabatic heating has been confirmed. It is quite possible that the combination of erosion and adiabatic heating result in some residual iron being fused to the target surface.

Cleaning of the surface layer. Single particle impact tests confirm that at higher velocities, erosion occurs and the surface oxide is cleaned from the target. This leaves a more reactive surface and dislocation networks that could act as diffusion pipelines for oxidation.

KEY FACTORS. Although all these factors could contribute to fatigue life behavior, it appears that the factors most likely to affect life capability based on these studies are:

- Beneficial compressive residual stress layer
- Detrimental plastic strain layer
- Change in true fracture strain (ductility capability)
- Surface roughness and effective surface stress concentration factor.

Of these factors, only the compressive residual stress layer is primarily characterized by peening intensity. Shot size, velocity, strain rate of the impact event, incidence angle, % coverage, and a variety of material properties control the other effects. Thus, shot peen intensity alone is inadequate for characterizing the peening process results from a life perspective.

Development of a Fracture Mechanics Model

Of the four factors identified as having the greatest potential life impact, the effects of the compressive residual stresses and increased surface roughness can be incorporated directly into fracture mechanics analysis. A residual stress profile can be incorporated into fracture mechanics analysis by linear superposition using a Green's function technique. The effect of surface roughness can be incorporated by defining a stress gradient which gives the effect of a stress concentration factor, or Kt, on the surface, but which decays to 1 with increasing depth. The effect of a detrimental plastic strain layer can be modeled using an initial flaw of some relevant size. This effectively assumes that there is a surface layer of some finite depth which has work-hardened to the extent that it behaves as a low ductility layer and will crack rather than undergo further plastic deformation. This is the most difficult element to quantify for the model. Since all specimens having a low life result showed semi-circular blue surface initiation sites (blue due to longer exposure to oxidizing environment at high temperature), an initial semi-circular flaw aspect ratio was selected. However, future work will also study the effect of shallower initial crack aspect ratios. Only the change in observed true fracture strain capability cannot be directly modeled using a fracture mechanics approach, however it is also possible that observed changes in material ductility may be adequately modeled using the assumption of an initial flaw.

Determination of initial flaw size. Several methods of determining the initial flaw depth were evaluated. The one providing the best correlation is the depth of slip observed in microstructures. This does represent the depth of plastic strain present in René 88DT, although this may not work for other alloys. Titanium, for example, is noted for undergoing adiabatic shear, resulting in a characteristic "white layer" or adiabatic shear layer.

Surface Roughness. Li, Mei, Duo and Renzhi [14] reported a method for estimating a geometric stress concentration factor due to specific surface roughness parameters, Rt (peak dimple depth) and S (dimple spacing) over some sample distance. Their work was based on extensive 3D seven-pit models, and a variety of other models. Since life behavior is governed by extremes (deepest dimple, highest Kt) a "max Kt" is employed instead of a mean Kt, by using the nominal Rt (peak depth) value plus three times the standard deviation of Rt. The equation for Kt (stress concentration factor) from Li is:

$$K_t = 1 + 4.0\left(R_{t_m} / S\right)^{1.3} \quad \text{, for } R_{t_m} / S < 0.15 \tag{3}$$

This behavior can be represented in a fracture mechanics analysis via a stress gradient. To model the decay away from the surface, an exponential fit with three times Rt as the decay depth for the Kt effect stress gradient is used, as shown in equation 4. Here, the decay distance of 3 times the peak dimple depth was chosen since 3 times a characteristic distance is often used as measure of when localized effects due to boundary conditions are no longer significant to bulk behavior.

$$\sigma(x) = (K_t - 1) \cdot e^{-x/(3 \cdot R_t)} + 1 \tag{4}$$

Like plastic strain, surface roughness is not a simple function of intensity. Shot size, velocity, incidence angle and % coverage appear to be significant factors.

Supporting evidence - from the Literature. A key assumption in this approach so far is the determination of an initial flaw size based on microstructure (or perhaps, that an initial flaw size can be defined which represents some state of work hardening or damage which correlates to life). Fortunately, significant support was found in the literature for the use of microstructure to characterize fatigue damage. Christ and Mughrabi [15] note that the fatigue of metals is a result of repeated cyclic plastic (or micro-plastic) deformation. The mechanisms of plastic deformation during cyclic loading correlates strongly with the microstructures, thereby determining the mechanisms of failure. Pangborn, Weissmann, and Kramer [16] observed that a propagating fatigue crack was formed whenever work hardening in the surface layer reaches a critical value. "When the barrier becomes sufficiently strong, fracture occurs if the local stress field exceeds the fracture strength. The remarkable extension of fatigue life resulting from surface removal is ascribed not to the removal of microcracks, but principally to the removal of the blocking effect due to the work hardened surface." Komotori and Shimizu [17] observe that the fatigue life in the extremely low cycle fatigue regime is primarily controlled by the mechanisms of work hardening and increase of internal micro-voids.

Zehetbauer [18] mentions that cold work hardening in stages IV and V of FCC metals involves statistical dislocation dynamics in terms of screw and edge dislocations and their specific interactions, and also allows for deformation-induced vacancies. Results suggest that: (a) type specific dislocation interaction determines the stress-strain relationships & evolution of dislocation density. (b) deformation induced vacancies play an important role. According to Zehetbauer, the formation of cell structure consists of: a) edge dislocations forming cell walls and b) congregation of screw dislocations in cell interiors. Vohringer [19] describes macro and micro residual stresses, and the dislocation mechanisms associated with both: a) micro stresses associated with plastic strain and seem to derive from the matrix dislocation structure, while b) macro stresses are associated with the wall / cell structure. Putting Zehetbauer and Vohringer together, it appears that:

- plastic deformation creates screw dislocations which reside in cell interiors
- macro residual stresses or "elastic" residual stresses are generated primarily by edge dislocations which comprise the cell walls.
- deformation which induces greater amounts of shearing action (oblique incidence angles) contributes a greater percentage of its energy to plastic deformation via introduction of screw dislocations.

Perhaps the real *coup de grace* comes from Burck, Sullivan and Wells [20] who studied the fatigue behavior of Udimet 700, a Nickel-base superalloy, when peened with glass beads. Burck et. al. employed slip band etching and cellular recrystallization to determine the extent of deformation generated by the peened layer. Consistent results were obtained, giving an average depth of about .002 inches for an intensity of 15N (equivalent of approximately 5A). They observed microcrack initiation at the surface along coherent annealing twin boundaries. Extrapolations conducted on linear crack length vs. number of cycles sometimes gave positive crack lengths at zero cycles, implying that the "cracks either initiated in finite lengths or that they initially grew at a rate much faster than in subsequent propagation." [20] Furthermore, crack initiation in peened material was similar to that for electropolished cases (except that it occurred at higher stress levels). "Once present, however, these small cracks grew at constant rates which were extremely slow compared to similar cracks in electropolished material." [20] However they noted that the propagation rates quickly approached those observed for the electropolished material as the cracks grew larger. This would be expected as the crack grows through the residual stress layer and is no longer influenced by it.

> "It should be noted that, in some cases, average crack propagation rates were less than one Burgers vector ($\mathbf{b} = 1.2 \times 10^{-8}$ in.) per cycle. This fact, together with the sudden appearance of crack segments at initiation, and the fourth power dependence of propagation rate on stress range tend to support a model of cumulative damage." [20]

While cold working of Udimet 700 had a large effect on tensile properties, they observed little effect on fatigue crack initiation or propagation at room temperature. Finally, Burck, Sullivan and Wells offer some specific insights on observed fatigue behavior of peened Udimet 700:

> "It appears then that much of the beneficial effect of glass bead blasting on the fatigue properties of Udimet 700 is derived from a very low rate of early crack propagation under the high compressive residual stress in the surface layer. A very important parameter in the case of Udimet 700 was the degree of blasting coverage. Although all specimens were bead blasted to Almen saturation, *i.e.*, until additional blasting time had little effect on measured Almen intensity, samples which were allowed additional blasting time apparently attained a more uniform stress distribution and showed a markedly improved fatigue strength. It should be noted however, that excessive bead blasting may cause the fatigue strengths of some materials to decrease and thus each material should be evaluated individually.
>
> The residual compressive stress apparently also prevented bead blast microcracks and carbide cracks in this material from propagating to failure." [20]

Supporting Evidence - Microstructural Observations. Figure 5 shows the microstructures and slip resulting from two different peening conditions: ccw14/10A/800% - 85° vs. 45° incidence angles. The density of slip observed for the 45° incidence angle is significantly greater than that observed for 85°, although the depth of observed slip is greater for the 85° impact. This suggests that the amount of plastic strain and screw dislocations induced by 45° impact is greater than that generated for 85° impact. This is also reflected in the plastic strain profiles of Figure 4. Microcracks were also found within the heavy slip layer for the specimen evaluated to date, as shown in Figure 6. This is further evidence in support of a low ductility work-hardened layer which may act to initiate a crack readily. Note that the concept of a "slip layer" or "damage layer" as proposed does not imply that the amount of "slip", "work-hardening" or "damage" is significant to the life behavior. There are clearly many peening conditions that result in consistently higher lives, and in fact this fracture mechanics method will often predict no crack growth for small flaw sizes where the calculated stress intensity factor is less than the threshold value.

Figure 6c shows an etched microstructure corresponding to those in which the microcrack was observed. This shows evidence of recrystallization beginning within some of the surface grains. Although the peening conditions resulting in the lowest lives did not have the deepest slip depth (as indicated in Figure 5, the 85° peened specimen edged the 45° specimen out on shear depth of slip), the Kt calculated for the 45° specimen was significantly higher.

Correlation of Fracture Mechanics Predictions with Shot Peen DoE Data

Figure 7 shows the correlation obtained with a subset of the DoE data, with and without the Kt stress gradient. In both cases, ***all surface initiations correlated within a factor of 2.*** This is considered to be good agreement for fracture mechanics, and accounts for some variability in material properties. This information is also summarized in Table 2. Shaded table cells indicate sub-surface initiations and above average life capability.

The failure initiation site of all of the remaining tests was subsurface. These specimens all had good lives. For the majority of these cases, fracture mechanics predicted that no crack growth would occur because the calculated stress intensity factor was below the threshold value. This is excellent because it correctly predicts the failure to be a fatigue initiation dominated event. When calculating component lives in applications, the lower of a fracture mechanics life and a fatigue life would likely be used. For those conditions in which fracture mechanics predicts no crack growth, the life estimate would be based on the fatigue life, which is conservative for the results obtained. There were a few cases in which the fracture mechanics method under-predicted the life capability of a specimen. This is conservative, and the results were still in line with the trends observed (i.e. still higher than lives predicted for the low life conditions). **This suggests that a fracture mechanics approach can be used as an effective lower bound estimate of life capability.**

Conclusions and Observations

- The results obtained are encouraging and suggest there is **strong evidence** for the use of a **fracture mechanics methodology as a lower-bound estimate of life capability.** Additional work is needed to evaluate the limitations of this approach, in terms of stress and temperature regimes, as well as sensitivity of the method to variations in any of the input parameters (residual stress profile, stress concentration

Figure 5: Comparision of 85° vs 45° incidence angle for CCW14, 10A, 800% peening condition (R88DT)

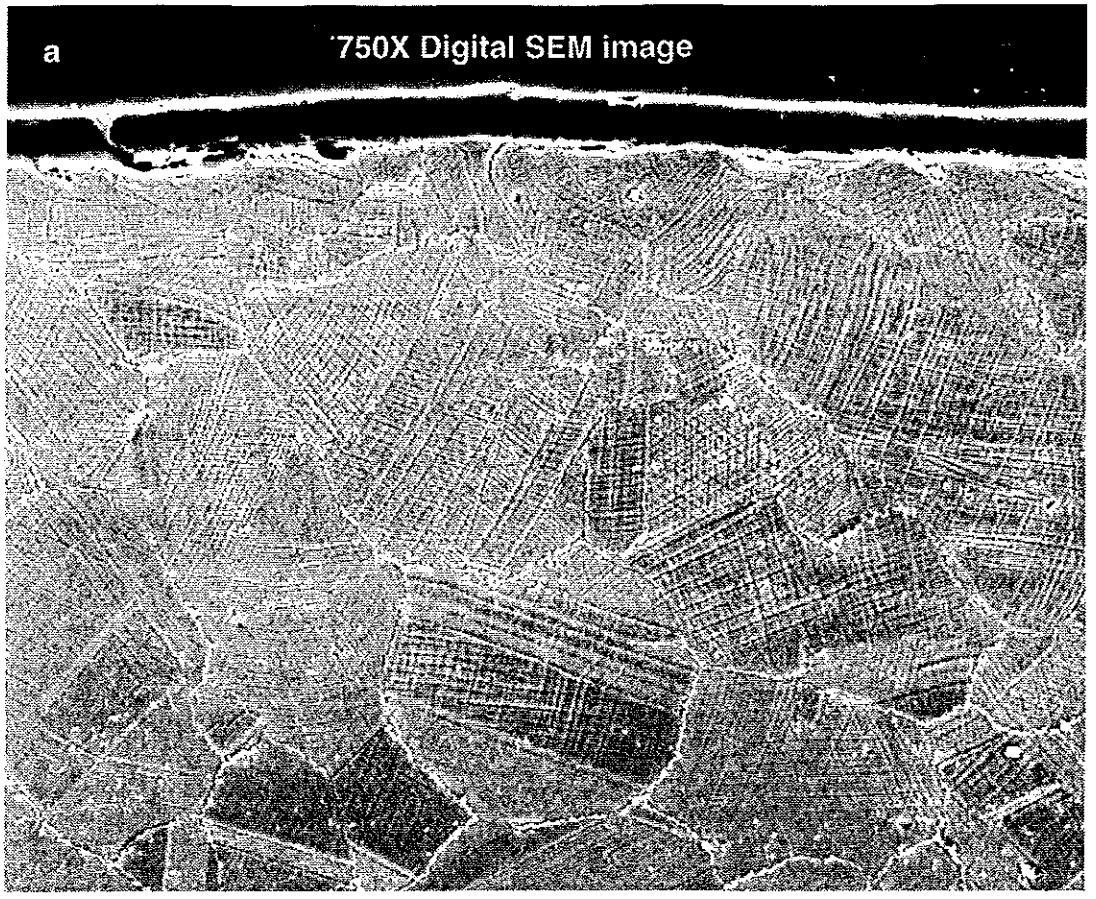

a) R88DT, ccw14, 10A, 85°, 800% coverage - slip layer depth=0.0025", Kt=1.25.

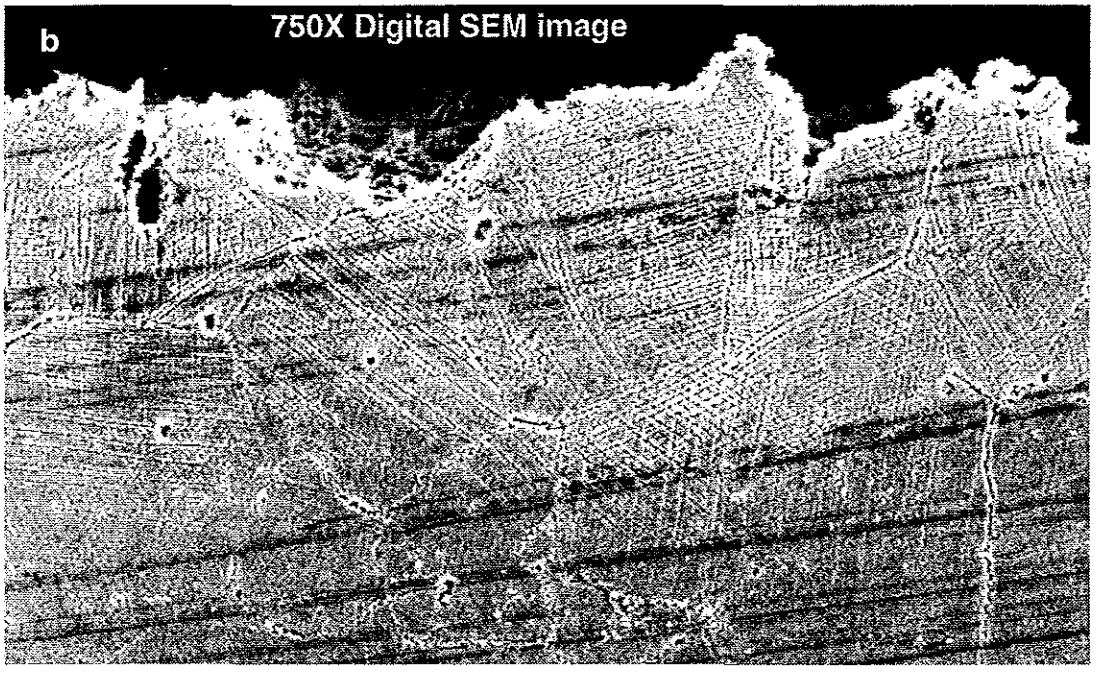

b) R88DT, ccw14, 10A, 45°, 800% coverage - slip layer depth=0.0019", Kt=1.47.

Figure 6: Microcrack Observation

R88DT, ccw14, 10A, 45°, 800%. a) & b) with 4 hour thermal exposure @1000°F. Microcrack dimensions ~ 2.3 μm x .2 μm, located approx. 41 μm below surface.

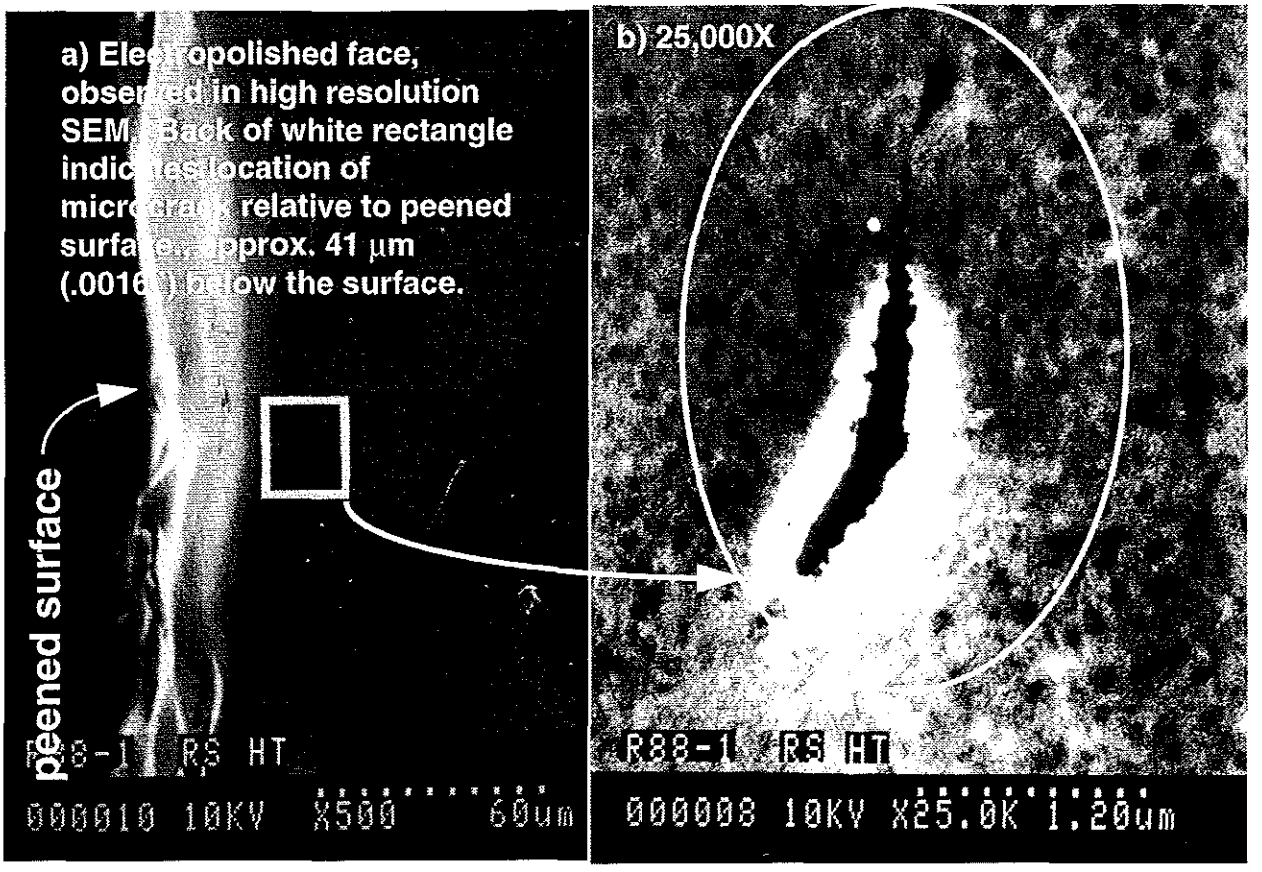

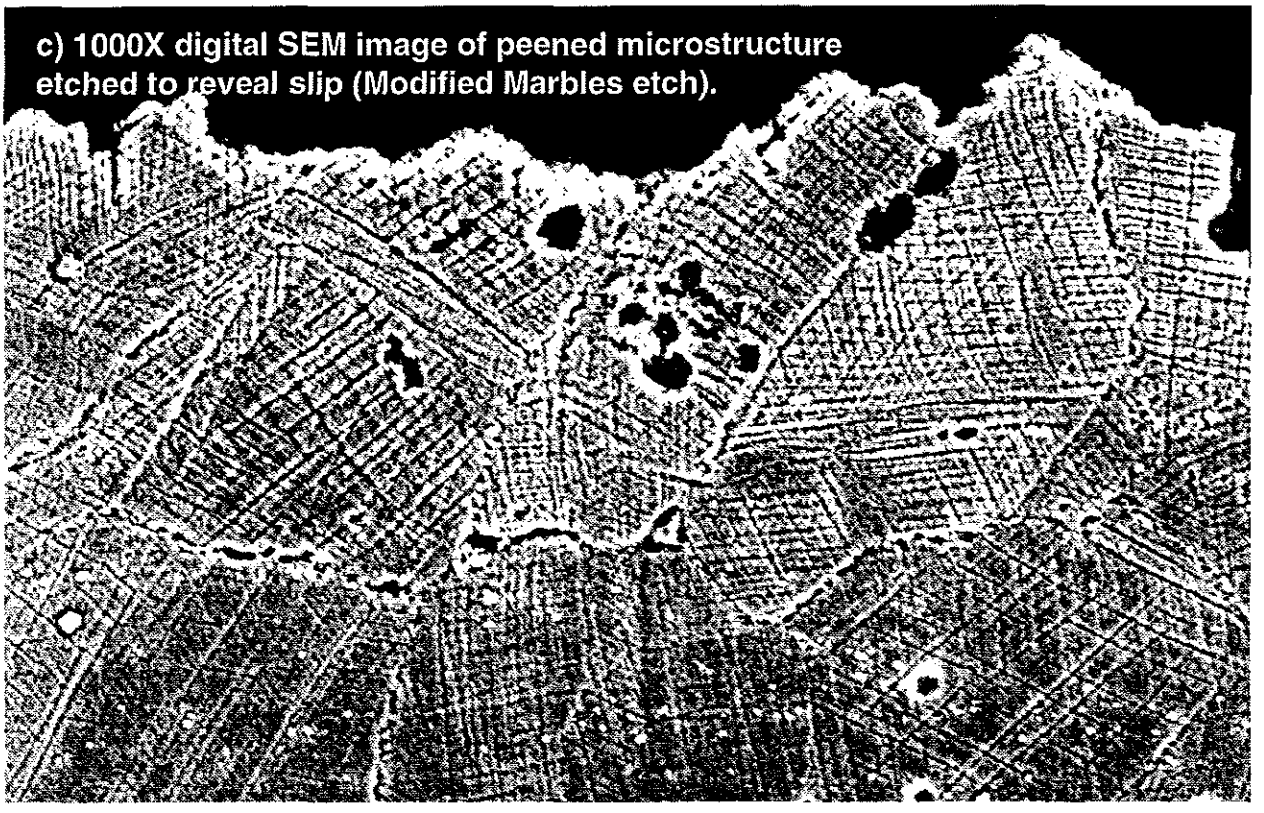

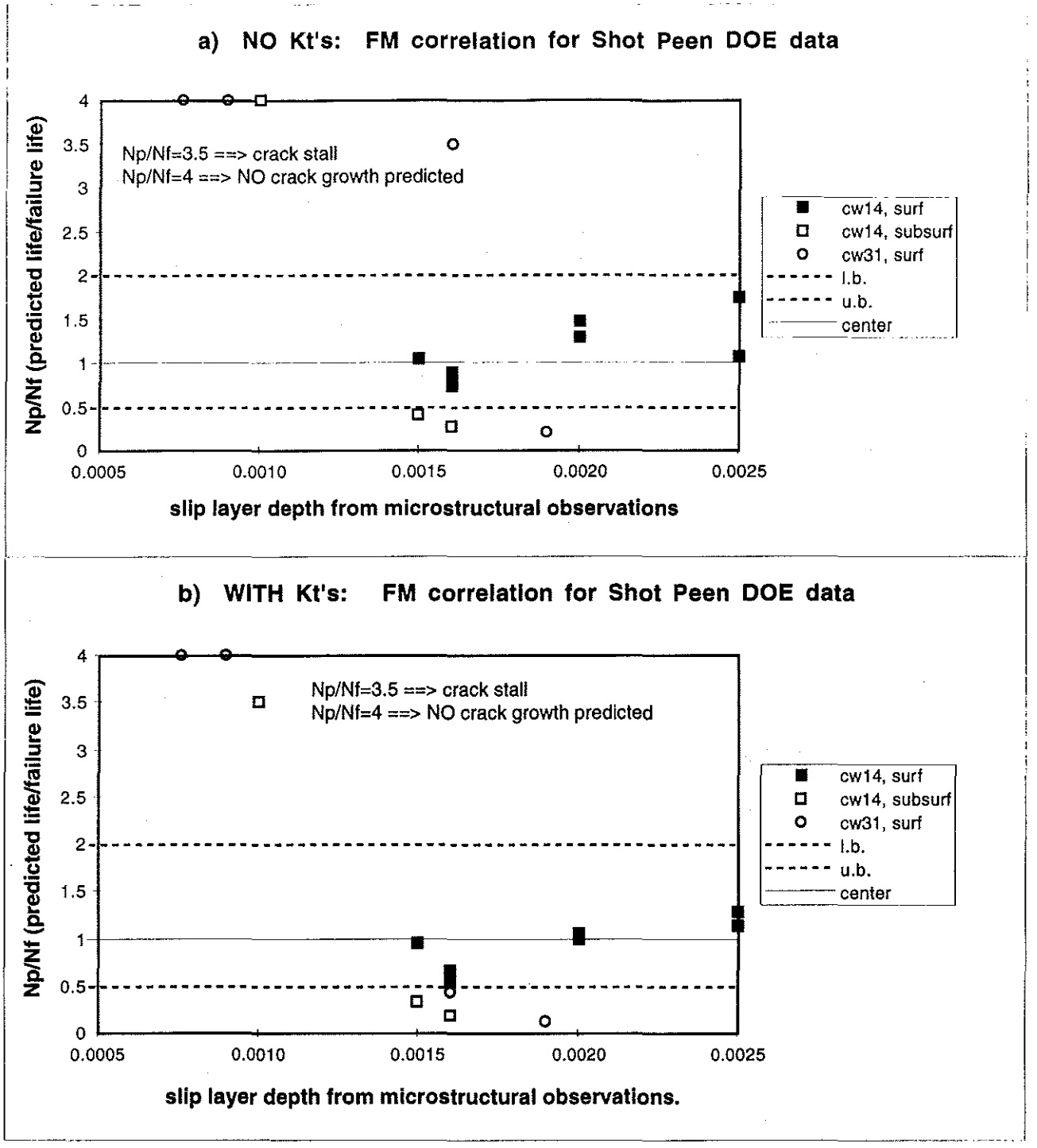

Figure 7: Fracture Mechanics correlations, with and without surface stress concentration factor / gradient

Use of a "Kt" stress concentration factor / strain gradient to model surface roughness effects improves life predictions for slip layer depths of ~.002" and greater.

Table 2: Summary of Microstructural Observations and Fracture Mechanics Correlations

Note that microstructural evaluation and slip depth determination was conducted on specimens peened several years after the original study. It is possible that more severe peening conditions were obtained for the ccw31, 10A, 45°, 800% peening condition, contributing to lower than normal life predictions.

									Np/Nf		Np	
shot	intensity mils "A"	angle	% cov	Kt	decay depth inches	Erosion mg/cm^2	Nf stdev	μstr damage depth inches	With Kt	No KT	With Kt	No KT
CCW14	6A	45	100%	1.29	0.0012		0.06					
			800%				-3.62					
		85	100%	1.31	0.0012	0.05	0.55	0.0010	3.5	4	crack stall	no growth
			800%	1.18	0.0008	0.03	-2.47	0.0016	0.54	0.74	21,305	29,256
							0.16	0.0016	0.19	0.27	24,876	36,588
	10A	45	100%	1.48	0.0021	0.13	-3.44	0.0016	0.65	0.9	17,677	24,601
									0.61	0.82	17,609	23,751
			800%	1.47	0.0019	1.49	-4.19	0.0020	1.06	1.47	21,526	29,801
									0.99	1.28	21,256	27,576
		85	100%	1.33	0.0014	0.05	-2.07	0.0015	0.94	1.04	46,555	51,714
							0.29	0.0015	0.34	0.4	47,411	55,826
			800%	1.25	0.0011	0.25	-4.00	0.0025	1.13	1.06	24,401	22,939
									1.28	1.73	28,651	38,501
CCW31	6A	45	100%	1.20	0.0009		0.32					
			800%				0.61					
		85	100%	1.17	0.0009	-0.01	0.14	0.0009	4	4	no growth	No growth
									3.5	4	crack stall	no growth
			800%	1.12	0.0006	-0.01	0.28	0.0016	0.44	3.5	64,351	stall
									0.65	3.5	81,551	stall
	10A	45	100%	1.25	0.0012		0.44	0.0008	4	4	no growth	No growth
									4	4	crack stall	no growth
			800%	1.23	0.0011		0.36	0.0019	0.14	0.21	20,351	30,076
									0.14	0.21	21,276	32,376
		85	100%				0.36					
			800%				0.20					

Shaded cells indicate a subsurface initiation. In general, the normalized life and microstructural slip depth are given for the peening condition. When significant variation exists between replications at a single condition, individual values are given for each replication (ccw14/6A/85°/800% and ccw14/10A/85°/100%).

factor, microstructural slip depth). Some of these effects can be estimated by conducting sensitivity studies on the input variables to the fracture mechanics code. Currently, determination of the "slip depth" from microstructures appears to have the greatest variability, in part due to the variability of microstructures themselves. Additional experience is needed to determine how sensitive the predictions are to these variations in the critical regimes of interest. This approach should also be evaluated for different alloys.

- Use of a **compressive residual stress profile, stress gradient** incorporating a surface roughness stress concentration factor, and an **initial flaw size** determined by **microstructural considerations** appears to be adequate for modelling purposes for a fracture mechanics calculation.

- This method could be used to **support "design to six sigma" objectives.** That is, information about component life requirements, geometry, and material considerations could be used to establish robust and cost-effective peening requirements up front in the design phase. Complex and expensive peening requirements could be streamlined without adversely affecting life capability. New peening conditions could be evaluated and "semi-optimized" in advance, resulting in more effective use of testing budgets.

- While the presence of "damaging" peening conditions was identified (where the term "damage" is used to indicate lives significantly lower than those obtained for average low-stress-ground specimens), the fact that the life results can be predicted using a fracture mechanics approach suggests that the benefit of the induced residual stress profile is still acting to delay crack propagation from surface defects. As long as an initial flaw size greater than or equal to the depth of slip for the peening condition is used, a fracture mechanics calculation can still provide a reasonable estimate of life capability.

Limitations to the current analysis and recommendations for further study.

As a result of this effort, two major conclusions and two recommendations surfaced:

1) The current definition of intensity [7] does not provide a unique characterization of the shot peening process. The only requirement is that a doubling of exposure time results in less than a 10% increase in intensity. Although this should ensure the condition selected is beyond the knee of the saturation curve, it doesn't prescribe where on the curve in relation to the knee. A more specific definition would assist in life correlation and process centering efforts.

2) Velocity, strain rate, incidence angle and shot size are all significant to characterization of the "detrimental plastic strain layer" induced. From an impact physics perspective, some direct characterization of velocity is needed to characterize the "slip depth" or plastic strain layer depth. The alternative is extensive testing and experimental correlations. Generation of saturation curves with velocity data could help clarify the relationship between shot size, velocity, incidence angle and intensity, improving confidence in life correlations.

3) In view of process variability and shift over time, the author recommends a 4 point saturation curve profile be requested at the onset of any shot peen test campaign,

along with a record of all machine settings and specific equipment used (machine type, nozzle type, robot arm, etc.) This would permit a regression curve fit to determine a more precise "intensity definition" and would permit comparisons with other peening conditions. Although this still will not capture variability in intensity measurements due to variability in the Almen strips themselves [21], it should help provide better documentation of the exact peening conditions used at that point in time.

4) Additional work is needed to characterize the variability in each of the input parameters (slip depth, surface roughness, residual stress profile), and the sensitivity of the analysis to those variations. The interaction of these effects could change over a range of test conditions and alloys. At this time, the most sensitive parameter appears to be the slip depth used for the initial crack size determination. It would be useful to obtain several microstructures for each shot peening condition being evaluated to provide a better characterization of the variability and depth of slip. Characterization of the microstructures for each peening condition used in new fatigue test campaigns is also important. One of the limitations of the current analysis is that there is no guarantee that the peened specimens produced several years after the original test are characteristic of the original peened specimens.

References

1 Tufft, Marsha K. 1996. "Instrumented Single Particle Impact Tests Using Production Shot: The Role of Velocity, Incidence Angle and Shot Size on Impact Response, Induced Plastic Strain and Life Behavior." Presentation given at the Sixth International Conference on Shot Peening, Sept. 4, 1996.

2 Wagner, L., G. Luetjering. 1981. "Influence of Shot-Peening on the Fatigue Behavior of Titanium Alloys" *First Int'l. Conf. on Shot Peening, Sept. 1981,* Pergamon Press, pp. 453-460.

3 Bailey, Pete. General Electric Aircraft Engines, Cincinnati, Ohio. Unpublished test results.

4 Abernethy, Robert B. 1993. *The New Weibull Handbook.* Published by Robert Abernethy, 536 Oyser Road, North Palm Beach, FL 33408-4328.

5 Niku-Lari, A. 1981. "Shot-Peening." *First Int'l. Conf. on Shot Peening, Sept. 1981,* Pergamon Press, pp. 395-403.

6 Verpoort, C.M., C. Gerdes. 1989. "Influence of shot peening on material properties and the controlled shot peening of turbine blades." *Shot Peening: Theory and Application,* John Eckersley & Jack Champaigne, editors. IITT International, pp. 11-70.

7 MIL-S-13165C, "Military Specification Shot Peening of Metal Parts." 7 June 1989, p. 11, ¶ 6.12.

8 VanStone, R. contribution to R83AEB650, *"F101-GE-102 B-1B Update to Engine Structural Durability and Damage Tolerance Analysis Final Report (ENSIP) Volume 2."* General Electric. p. 5-2-2.

9 Hutchings, I.M. 1979. "Energy absorbed by elastic waves during plastic impact." *J. Phys. D: Appl. Phys.*, Vol. 12, 1979, pp. 1819-1824.

10 Henning, C., D. Mewes. 1995. "Visualization of surface waves propagating over surfaces eroded due to particle impact." *Proc. of 8th Int'l Conf. on Erosion by Liquid and Solid Impact.* pp. 78-85.

11 Finnie, Iain. "The mechanism of erosion of ductile metals." *ASME, Proc. 3rd U.S. Natl. Congress of Applied Mechanics, 1958,* pp. 527-532.

12 Hall, E. 1993. Unpublished work. General Electric Corporate Research and Development Center, Schenectady, NY.

13 Renzhi, Wang, Zhang Xuecong, Song Deyu, Yin Yuanfa. 1981. "Shot peening of superalloys and its fatigue properties at elevated temperature." *First Int'l. Conf. on Shot Peening,* Sept. 1981, Pergamon Press, pp. 395-403.

14 Li, J.K. Yao Mei, Wang Duo, Wang Renzhi. 1992. "An analysis of stress concentrations caused by shot peening and its application in predicting fatigue strength," *Fatigue and Fracture of Engineering Materials & Structures,* Vol. 15, No. 12, Dec. 1992, pp. 1271-1279.

15 Christ, H.-J., H. Mughrabi. 1992. "Microstructure and Fatigue." *Low Cycle Fatigue and Elasto-Plastic Behavior of Materials - 3.* K.T. Rie, editor. Elsevier Applied Science: New York, pp. 56-69.

16 Pangborn, R.N., S. Weissmann, I.R. Kramer. 1979. "Prediction of Fatigue Life by X-Ray Diffraction Methods." *Fatigue Fract. Engng. Mater. Struct.* Vol. 1, No. 3, pp. 363-369.
17 Komotori, Jun and Masao Shimizu. 1992. "Microstructural Effect Controlling Exhaustion of Ductility in Extremely Low Cycle Fatigue." *Low Cycle Fatigue and Elasto-Plastic Behavior of Materials - 3.* K.T. Rie, editor. Elsevier Applied Science: New York, pp. 136-141.
18 Zehetbauer, M. 1993. "Cold Work Hardening In Stages IV And V Of F.C.C. Metals - II. Model Fits And Physical Results." *Acta. metall. mater.* Vol. 41, No. 2, pp. 589-599.
19 Vohringer. 1994. "Surface residual stress relaxation in steels by thermal mechanical treatment." *Proceedings of the Fourth International Conference on Residual Stresses,* Society for Experimental Mechanics, Inc. pp. 598-607.
20 Burck, L.H., C.P. Sullivan, C.H. Wells. 1970. "Fatigue of a glass bead blasted Nickel-base superalloy." *Met. Transactions,* v 1, June 1970, pp. 1595-1600.
21 Happ, Marvin B., David L. Rumpf. 1996. "Almen Strip Variability - A Statistical Treatment." *Sixth International Conference on Shot Peening.*

Acknowledgments

This work has built upon the significant work and contributions of others who share my enthusiasm for shot peening. I would particularly like to acknowledge the help and contributions of Pete Bailey, Herb Popp, Bill Ross, Dale Lombardo, Paul Domas, Mike Lasonde, Marv Happ, Bob Thompson, Chip Blankenship, Mike Henry, Marek Winairz, Ralph Somers, Floyd Brate, Bill Davis, Paul Follansbee, Jim Williams and Robyn Brands from GE. I would also like to thank Dr. Joe Gallagher, Dr. Gordon Sargent, Dr. Daniel Eylon, Dr. Jim Snide, Dr. Gerald Shaughnessy, Dr. N. Singh Brar, Dr. Terry Murray and Dr. Bob Brockman from the University of Dayton, and Dr. Alan Zehnder from Cornell University, who have provided great guidance and assistance in this effort.

Footnote

The first rough fracture mechanics calculations were conducted in January 1996, as a result of the microstructures obtained of precision sections through impact dimples from the single particle impact test completed in November-December, 1995 [1]. However, the exclusion of a Kt factor at that time did not permit adequate differentiation between the 45° and 85° incidence angle effects. Around this time, Herb Popp, working independently, advocated the use of a fracture mechanics approach and suggested iterating to find what size cracks were needed to correlate with test data. The next round of iterations focused on the plastic strain profile, and an attempt to define a "damage depth" as the layer above which the compressive plastic strains exceeded a critical plastic strain (perhaps the true fracture strain for the peening condition of interest). Although this method also obtained results of the right order of magnitude, it did not predict the right trends to differentiate between peening treatments. The team advised caution in trying to interpret and apply the plastic strain information obtained from x-ray diffraction techniques as well as "true fracture strain" data from tensile tests in terms of cyclic strain. At this point, the work of Li, Mei, Duo and Renzhi [14] on surface roughness was retrieved and incorporated into the analysis. This improved the correlation, but still did not reverse some of the inconsistent trends. Finally, the plastic strain/true fracture strain approach was abandoned and the microstructural slip measurements were retrieved and incorporated into the model with the custom residual stress profiles and Kt stress gradients for the first time. This combination provided the differentiation between peening conditions which was sought. The only exception is the overly pessimistic prediction of the ccw31/10A/45°/800% condition life.

If further investigation confirms the connection between microstructural slip depth and life capability, then the effect of specific shot peening process conditions on complex features such as corners, holes and fillets could be evaluated directly by taking surface roughness measurements and obtaining microstructures through a sample feature. This would provide a direct method which does not depend on a lengthy list of questionable assumptions. Alternately, regression analysis could be used to correlate the effects of intensity, % coverage, % saturation, incidence angle, velocity, shot size and hardness.